International Research Journal of Engineering and Technology (IRJET) e-ISSN: 2395-0056
Volume: 10 Issue: 07 | Jul 2023 www.irjet.net p-ISSN: 2395-0072

Experimental Investigation of Faults in Roller Element Bearing Using Vibration Based Method

Shankar G. Rane[1], Jayesh R. Satam[1], Prasad R. Mejare[1], Hrutik M. Salkar[1], S. S. Kulkarni[2]

1- Students, Dept. of Mechanical Engineering, SSPM College of Engineering, Kankavli, Maharashtra, India.
2- Dept. Mechanical Engineering, SSPM College of Engineering, Kankavli, Maharashtra, India.

Abstract - *The development of small, localized pits causes distributed faults in rolling element bearings. This raises the cost of maintaining industrial machinery by causing rotor systems to fail prematurely or even catastrophically if not promptly monitored. This study proposed a technique for diagnosing rolling element bearings using vibration analysis (VS) to find distributed problems. The internal experimental test rig was created and constructed to allow for the experimental investigation of the vibrational properties of distributed faults. Analytical models are contrasted with experimental outcomes. Here, the threshold life of any bearing may be predicted after the introduction of the flaw.*

Here, localized and spread defects are compared, and the vibrational signatures of both are correlated with healthy bearings. This study offers a method for estimating the bearing life following the introduction of a fault.

Key Words: *Bearing failure, life of bearing, vibration-based analysis, etc.*

1.INTRODUCTION

The number of rotations a bearing can withstand before failing due to rolling fatigue or failure of the inner ring, outer ring, or rolling element (ball or roller) are two ways that the service life of a bearing is stated. When equipment or a machine component fails under the prescribed conditions of use as stipulated by its manufacturer, it is said to have reached the end of its rated life. The bearing's service life is different from its rated life because it may fail due to improper lubrication, misalignment, and mounting damage before it reaches its real life.

The bearing's mounted accelerometer collects data, which is then analyzed on an FFT analyzer. Separating undesired data from other energy sources within the machine is a crucial component of processing. By incorporating selective digital filtering into the software, this is accomplished. In this study, data from damaged and undamaged bearings are compared to pinpoint the flaw. After a set amount of time, the bearings are regularly monitored to see if they are operating within acceptable limits.

2. EXPERIMENTATION

The proposed experimental setup shown in fig. no.2 is rotor bearing system used for study. Numbers of experiments were executed and validated with Analytical results.

2.1. Design of Setup - Calculation:

To apply same loading condition, we choose disc of steel with diameter 150 mm and thickness having 5 mm.

D = 150 mm
t = 5 mm
$V = \pi/4*(r^2)\ t$
$= \pi/4*(0.075^2) *0.005$
$= 0.0000221\ m^3$
P = m\v
m = ρ*v = 7850*0.0000221 = 0.1735 N
m = 1.702 kg
F = m*g = 1.702*9.81 = 16.69 N
Ƈ = F*L = 16.697*0.29
Here L = 0.29m
Ƈ = 4.84 Nm
P = 2πNƇ/60
P = 2π*1440*4084/60
P = 729.85 W
P = 0.72985 KW
P = 0.978 hp

Therefore, we select motor having 1 HP power and 1440 RPM.

Shaft Calculation:

Power of Motor P = 1 Hp = 0.746 Kw
N = 1440 rpm
Syt value of steel = 265 N/mm^2
FOS (Factor of Safety) = 3
σ_t = Syt/FOS
=265/3
σ_t =88.33 N/mm^2
Ƈ = 0.5Syt/FOS
=0.5×265/3
Ƈ =44.165 N/mm^2

A) Shaft is subjected to pure bending load:

$\sigma_t = \sigma_b = M_b \times Y / I$
$= M_b/(\pi/64)d^4 \times (d/2)$

$\sigma_t = M_b/(\pi/32)d^3$
$M_b = 180 \times 16.69/2$
$M_b = 1502.1$ N/mm²
$d = (M_b/(\pi/32)\sigma_t)^{1/3}$
$= (1502.1/(\pi/32)88.33)^{1/3}$
$d = 13.161$ mm

B) Shaft subjected to Torsion moment:

$C = (Mt/J) \times R$
$R = d/2$
$Mt = (P \times 60 \times 10^6)/(2\pi N)$
$= (0.746 \times 60 \times 10^6)/(2\pi \times 1440)$
Mt = 4947.06 Nmm
$C = [Mt/(\pi/32)d^4] \times (d/2)$
$C = 16Mt/\pi d3$
$d = (16 \times 4947.07/\pi \times 44.165)$
d = 8.29 mm

From this we selected 20 mm diameter of rod.

The experiments are performed at 1440 rpm rotor speed and 16.7 N radial load. The length of the shaft for the rotor bearing system is 290mm, and diameter of the rotor is 20mm. the shaft is supported by two bearing (bearing number: UCP204) at the drive and non-drive end.

The rotor speed is varied by Dimmerstat. the condition of the bearing mounted towards loading arrangement side is monitored by using an accelerometer. Bearing under test is placed at this position only. The accelerometer is placed right above the bearing casing perpendicular to the axis of the rotation of the shaft in such a way so that it can acquire vertical acceleration.

Vibration analysis by using FFT analyzer and the software named is T-ViB sound and vibration analysis software has been used for the frequency analysis of the bearings.

2.2. Experimental Setup

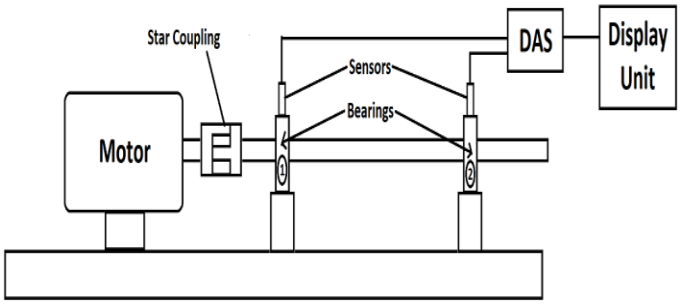

Fig. no-1: Block diagram of bearing test rig

Fig. no-2: Bearing test Rig

2.3. INSTRUMENTS USED FOR EXPERIMENTATION

2.3.1. Sensor – Piezo-Electric Accelerometer:

Piezo-Electric accelerometer is used as sensor. It is an accelerometer that employs the piezo electric effect of certain material to measure dynamic changes in mechanical variables (Ex. Acceleration, vibration, and mechanical shock).

Using the general sensing method upon which all accelerometers are based, acceleration acts upon seismic mass that is restrained by a spring or suspended on a cantilever beam and converts a physical force into an electrical signal. Before the acceleration can be converted into an electrical quantity it must first be converted into either a force or displacement.

2.3.1.1. Specifications

Accelerometer: S/N 372662
Sensitivity: 95.51 mV/g
BIAS: 12.06 V

Fig. no-3: Accelerometer (Sensor)

2.3.2. DAS (Data Acquisition System) – FFT Analyzer:

Data acquisition is the process of sampling signals that measures real-world physical condition and converting resulting sample into digital numerical values that can be manipulate by computer.

Fig. no-4: FFT Analyzer

2.3.3. Display Unit:

It displays the data in digital format. T-ViB sound and vibration analysis software is used.

Fig. no-5: Display Unit

3. ANALYTICAL ESTIMATION OF DEFECT FREQUENCIES

To calculate Defect frequencies of Antifriction Bearings we required

N = 1440 rpm
d= 7.94 mm (diameter of ball of bearing)
P= 17.28×2=34.58 mm
Z= 8 (no. of balls of bearing)
α = 0 (helix angle)

1) Inner race defective frequency (Fdi)
   Fdi = (ZN/2) × (1+(d/P) cosα)
   = (8×1440/2) × (1+(7.94/34.56) cos0)
   =7083.33 cpm
   =118.055 Hz

2) Outer race defective frequency (Fdo)
   Fdo = (ZN/2)×(1-(d/P) cosα)
   = (8×1440/2) × (1-(7.94/34.56) cos0)
   = 4436.67 cpm
   = 73.94 Hz

3) Rolling element defective frequency (Fdr)
   Fdr = (PN/2d) × (1-(d/P)^2 cos^{2}α)
   = (34.56×1440/2×7.94)
   × (1-(7.94/34.56)^2 cos^{2}0)
   = 2968.49 cpm
   = 49.47 Hz

4) Cage defect = 1.5×N
   = 1.5×1440
   =2160 cpm
   = 36 Hz

4. RESULT AND DISCUSSION

Here are some images of the readings we got during the experimentation:

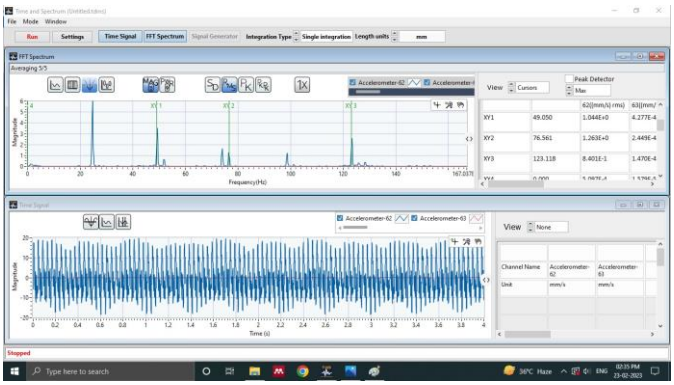

Fig. no-6: 5 Hour reading

Here (Fig. no-6) cursor is kept on 49.05 (roller element defect), 76.56 (outer race defect) and 123.118 (inner race defect) for which we get 1.044 mm/s, 1.263 mm/s and 0.84 mm/s values of amplitude respectively.

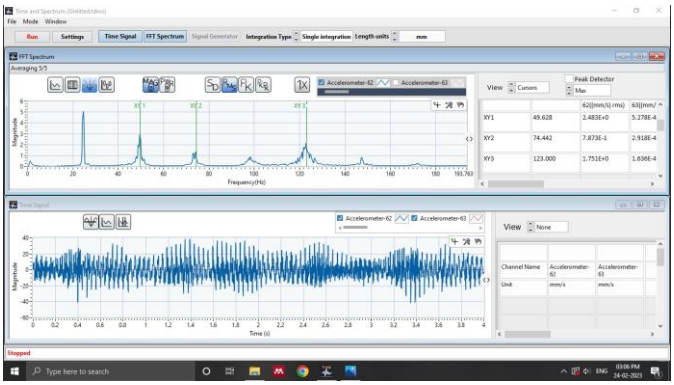

Fig. no-7: 10 Hour reading

Here (Fig. no-7) cursor is kept on 49.62 (roller element defect), 74.44 (outer race defect0 and 123 (inner race defect) for which we get 2.48 mm/s, 0.78 mm/s and 1.75 mm/s values of amplitude respectively.

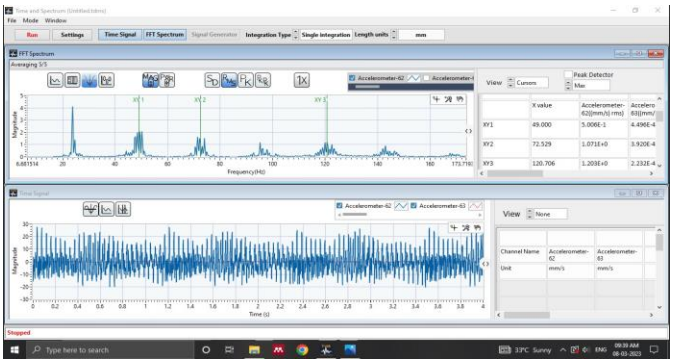

Fig. no-8: 15 Hour reading

Here (Fig. no-8) cursor is kept on 49 (roller element defect), 72.52 (outer race defect) and 120.70 (inner race defect) for which we get 0.50 mm/s, 1.07 mm/s and 1.20 mm/s values of amplitude respectively.

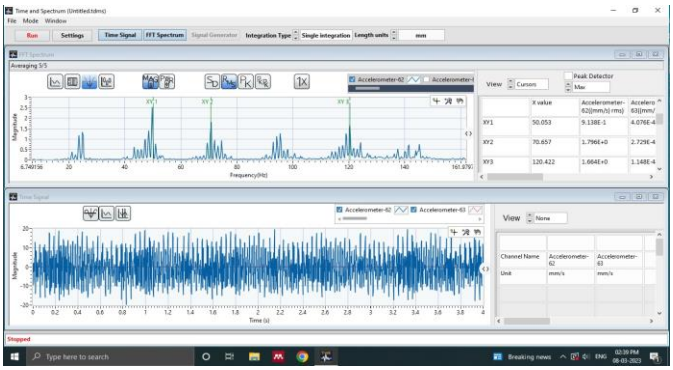

Fig. no-9: 20 Hour reading

Here (Fig. no-9) cursor is kept on 50.05 (roller element defect), 70.65 (outer race defect) and 120.44 (inner race defect) for which we get 0.91 mm/s, 1.79 mm/s and 1.66 mm/s values of amplitude respectively.

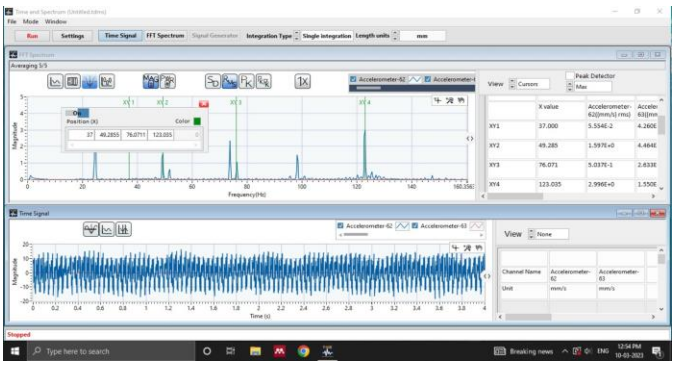

Fig. no-10: 25 Hour reading

Here (Fig. no-10) cursor is kept on 49.28 (roller element defect), 76.07 (outer race defect) and 123.035 (inner race defect) for which we get 1.59 mm/s, 0.50 mm/s and 2.99 mm/s values of amplitude respectively.

Here the Upper graph represents frequency domain and lower one represents time domain graph.

For our experimentation we have considered frequency domain graph on which x axis it represents magnitude and y axis represents frequency (hz).

The 3-defected frequency which we calculated for roller element, outer race defect and inner race defect are 49.47 Hz, 73.94 Hz, 118.055 Hz respectively. In Frequency domain graph XY1 peak represents roller element defect, XY2 peak represents outer race defect and XY3 peak represents inner race defect so according to it we put the cursor on the following points and obtained amplitude peaks for them. As the defect is been introduced to bearing 2 (Fig-2) so readings are obtained from accelerometer 62 which connect to FFT channel A. To get precise value 5 times averaging is done which are superimposed on each other.

Inner race defect (frequency 123.035Hz)

X	Y	D	D*Y	D*D
5	0.841	-2	-1.682	4
10	1.751	-1	-1.751	1
15	1.203	0	0	0
20	1.664	1	1.664	1
25	2.99	2	5.98	4
5	8.449	0	4.211	10
a	1.6898			
b	0.4211			

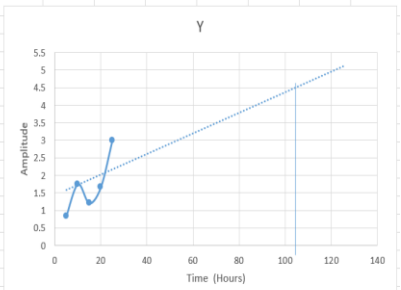

Chart no-1: Inner race defect

The values obtained from the experimentation a graphical representation is done in which x-axis represents hrs. which is independent function and y-axis represents frequency which is dependent.

From fig. no1[2] we studied that different satisfactory and unsatisfactory conditions of vibrations of bearing which divided into four classes. From fig. no1[2] Vibration Severity ISO10816 we came to know that 4.5 mm/s there is a defect which cannot be prevent. So, after that condition we change the bearing.

3 different graphs are plotted for 3 different defects. after plotting the graph least square method is used to predict the future points.

least square method is nothing but a statistical procedure to find the best fit for a set of data points by minimizing the sum of the offsets or residuals of points from the plotted curve.

Least squares regression is used to predict the behavior of dependent variables. After finding the best fit line a progression of line from 4.5 mm/s amplitude is done on best fit line the graph point at which intersection occurs from three there a strain projection on x axis that is hr. is done which done which can called as threshold life of bearing that is the of hr. of times up to which bearing can still be used after been used defect is occurred.

6. CONCLUSIONS

Generally, what everyone does that once that the defect in bearing is detected the company replaces the bearing with new one but from our study, we came to know that immediately replacement of bearing is not necessary.

In our study we purposefully introduced the defect on inner race and carried the experiment and form we came to know that even if the defect is introduced the bearing still can be used for approx. 104 hrs. safely.

But here some unwanted noise occurs. Which can be removed by proper lubricant which eventually increases its life.

REFERENCES

[1] R. K. Upadhyay, L. A. Kumaraswamidhas, and M. S. Azam, "Rolling element bearing failure analysis: A case study," *Case Stud Eng Fail Anal*, vol. 1, no. 1, pp. 15–17, Jan. 2013, doi: 10.1016/j.csefa.2012.11.003.

[2] B. Artono, A. Susanto, and N. A. Hidayatullah, "Design of Smart Device for Induction Motor Condition Monitoring," in *Journal of Physics: Conference Series*, IOP Publishing Ltd, Mar. 2021. doi: 10.1088/1742-6596/1845/1/012035.

[3] D. Kumar Prasad, M. Amarnath, and H. Chelladurai, "An experimental approach to study the effect of wear on traction coefficient and dynamic response of roller bearing," in *Materials Today: Proceedings*, Elsevier Ltd, 2019, pp. 9889–9892. doi: 10.1016/j.matpr.2021.01.408.

[4] E. Wescoat, L. Mears, J. Goodnough, and J. Sims, "Frequency energy analysis in detecting rolling bearing faults," Elsevier B.V., 2020, pp. 980–991. doi: 10.1016/j.promfg.2020.05.137.

[5] G. L. Suryawanshi, S. K. Patil, and R. G. Desavale, "Dynamic model to predict vibration characteristics of rolling element bearings with inclined surface fault," *Measurement (Lond)*, vol. 184, Nov. 2021, doi: 10.1016/j.measurement.2021.109879.

[6] L. Renaudin, F. Bonnardot, O. Musy, J. B. Doray, and D. Rémond, "Natural roller bearing fault detection by angular measurement of true instantaneous angular speed," in *Mechanical Systems and Signal Processing*, Academic Press, 2010, pp. 1998–2011. doi: 10.1016/j.ymssp.2010.05.005.

[7] L. H. Zhao, Q. C. Li, J. Z. Feng, and S. L. Zheng, "Service life prediction method for wheel-hub-bearing under random multi-axial wheel loading," *Eng Fail Anal*, vol. 122, Apr. 2021, doi: 10.1016/j.engfailanal.2020.105211.

[8] J. Viola, Y. Q. Chen, and J. Wang, "FaultFace: Deep Convolutional Generative Adversarial Network (DCGAN) based Ball-Bearing failure detection method," *Inf Sci (N Y)*, vol. 542, pp. 195–211, Jan. 2021, doi: 10.1016/j.ins.2020.06.060.

[9] J. Park, S. Kim, J. H. Choi, and S. H. Lee, "Frequency energy shift method for bearing fault prognosis using microphone sensor," *Mech Syst Signal Process*, vol. 147, Jan. 2021, doi: 10.1016/j.ymssp.2020.107068.

[10] N. W. Nirwan and H. B. Ramani, "Condition monitoring and fault detection in roller bearing used in rolling mill by acoustic emission and vibration analysis," in *Materials Today: Proceedings*, Elsevier Ltd, 2021, pp. 344–354. doi: 10.1016/j.matpr.2021.05.447.

[11] R. Kumar and M. Singh, "Outer race defect width measurement in taper roller bearing using discrete wavelet transform of vibration signal," *Measurement (Lond)*, vol. 46, no. 1, pp. 537–545, 2013, doi: 10.1016/j.measurement.2012.08.012.

[12] P. Maurya, N. Mulani, C. Michael, and D. Jebaseelan, "Failure Analysis of Drive Axle Shaft failed under Torsional Stress," *IOP Conf Ser Mater Sci Eng*, vol. 1128, no. 1, p. 012011, Apr. 2021, doi: 10.1088/1757-899x/1128/1/012011.

[13] P. K. Kankar, S. C. Sharma, and S. P. Harsha, "Fault diagnosis of rolling element bearing using cyclic autocorrelation and wavelet transform," *Neurocomputing*, vol. 110, pp. 9–17, Jun. 2013, doi: 10.1016/j.neucom.2012.11.012.

[14] M. S. Rao, "Reliability Analysis based Condition Monitoring of Process Equipments," 2017. [Online]. Available: www.internationaljournalssrg.org

[15] N. D. Dhote *et al.*, "A Case Study-Failure of Roller Spherical Bearing of Shakeout Used In Foundry Industry," 2014. [Online]. Available: www.ijesi.org

[16] P. M. Jadhav, S. G. Kumbhar, R. G. Desavale, and S. B. Patil, "Distributed fault diagnosis of rotor-bearing system using dimensional analysis and experimental

methods," *Measurement (Lond)*, vol. 166, Dec. 2020, doi: 10.1016/j.measurement.2020.108239.

[17] V. G. Salunkhe, R. G. Desavale, and T. Jagadeesha, "A numerical model for fault diagnosis in deep groove ball bearing using dimension theory," in *Materials Today: Proceedings*, Elsevier Ltd, 2021, pp. 3077–3081. doi: 10.1016/j.matpr.2021.06.072.